

# Numerical and Experimental Study of Natural Convection Air Flow in a Solar Tower Dryer

Germain W. P. Ouedraogo<sup>1</sup>, Sié Kam<sup>1</sup>, Moussa Sougoti<sup>1</sup>, Ousmane Moctar<sup>1,2</sup>, Dieudonné Joseph Bathiebo<sup>1</sup>

<sup>1</sup>Physic Department, Ouaga 1 University Professor Joseph Ki-Zerbo, Ouagadougou, Burkina Faso

<sup>2</sup>University of Agadez PO BOX 199 Niger

**Abstract**— This work focuses on the study of the flow of air in natural convection in a solar tower of small size. The behavior of air in the tower, considered as a solar dryer, provides information on the amount of heat absorbed by the air upon entry into the collector. A theoretical approach allows us to theoretically simulate the flow by using a mathematical model characterizing the physical parameters of the system during a daily sunshine. An analysis of this phenomenon is made and results are obtained.

**Keywords**— Flow of air, natural convection, solar tower, dryer.

## I. INTRODUCTION

The concept of solar tower or solar power chimney was proposed first by Cabanyes [1]. Solar towers consist of a collector, a chimney and a turbine. They allow the production of electricity. A Solar tower without its turbine can have a use other than that of power generation: the drying of food products, thanks to the drying air coming out of its collector; hence its name of solar tower dryer.

The drying of food products is an appropriate means to curb losses of food after harvest and expand the consumption of these products during periods of non-production. This is an operation which is much practiced in West Africa by farmers. Several studies have shown the difficulty of getting indisputable elements of validation and comparison between different solar dryer models due to its technological diversity.

In our work, we study the operation of a solar tower dryer, running empty. The objective is the use of the energy gain received by the air through the collector for the drying of food products. To do so, it is essential to carry out a study of fluid flow in the system in order to know the amount of energy that the air must absorb with an average humidity of 40% in the cases of BURKINA FASO.

## II. DESCRIPTION OF THE SOLAR TOWER DRYER

The solar tower dryer is a natural thermal power generator, which uses solar radiation to increase the internal energy of the air flowing in its collector. The useful gain of the solar collector is converted into kinetic energy flow circulating in the chimney where trays or racks are arranged.

### 2.1. Description of the solar tower

As part of our work, the solar tower has a function other than to produce electricity. Used as solar dryer, it is small compared to that producing electricity and consists mainly of a collector and a chimney.

- The collector has a radius of 1.2 meters. This is the part where the air circulates. It is heated by absorption of solar flux and subjected to phenomena of convection. The collector consists of a cover of four square shaped glass windows of a square meter and an absorber in alu-zinc painted matte black, between which the air flows.
- The chimney has a diameter of 0.4 meters and a height of 3 meters; it is the drying chamber and has racks for display of products to dry. The chimney has two roles: that of drying-chamber and that of drawing of drying air. The greater its height, the more important its pull effect and it promotes the renewal of air in the [2-3] system.

### 2.2. Functioning of the solar dryer

The products to be dried are not directly exposed to solar radiation and that makes of the tower an indirect solar dryer. The air entering the collector is heated by natural convection from the sensor and moves through the chimney effect towards the drying chamber where the drying air takes away the water molecules from the products to be dried ( Fig.1).

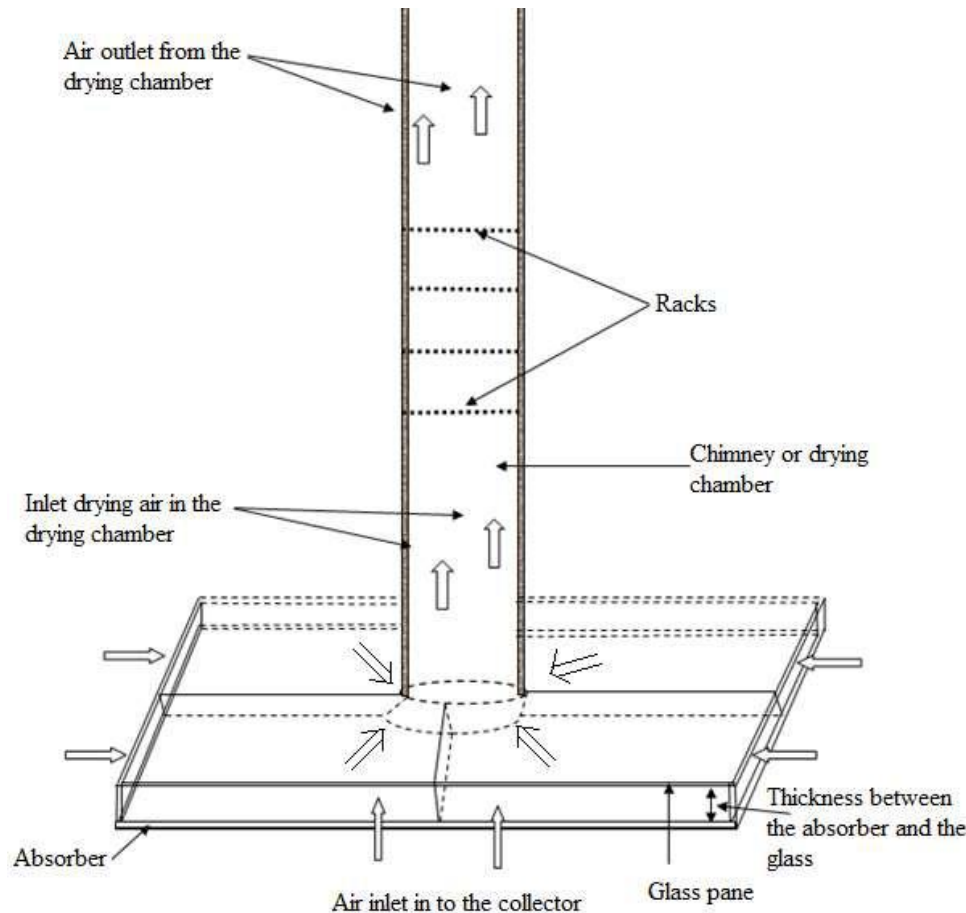


Fig.1: Diagram of the experimental solar tower dryer

### III. MATHEMATICAL MODELING OF THE AIR FLOW IN THE SOLAR TOWER DRYER

The solar dryer is said to be empty when the drying chamber does not contain any products. The modeling consists in transcribing physical phenomena that can be observed and equations that can arise at different levels of the system.

#### 3.1. Simplifying assumptions

The study of heat transfer in the system can be simplified by assuming:

- A uni-dimensional flow depending on an average radius in the chimney and the height in the chimney.
- Properties of the air such as dynamic viscosity, thermal conductivity, density and heat capacity that are considered constant.
- The air follows the Boussinesq approximation rules, which results in the expression:  
 $\rho = \rho_0[1 - \beta(T - T_0)]$   
 with  $\beta = \frac{1}{T_0}$
- Transfer by conduction of the sensor (absorber) is negligible as it is a thin metal and its conductivity

coefficient is very high; the temperatures of these two faces are therefore uniform.

- The heat transfer by conduction through the glass pane is negligible because it has a small thickness; the two sides have substantially the same temperature when the glass is exposed to sunlight.
- The radiative exchanges of air are negligible.

#### 3.2. Equation governing the flow of air in the system

The rectangular collector is considered circular for its modeling in the system of polar coordinates. The equations of the air flow are a function of the radial axis  $r$ . In the chimney, the equations are a function of the axial axis  $z$ .

##### 3.2.1. Continuity equation

In natural convection, air velocity is 'a priori' unknown. So we assume that the air flow is constant in the system.

$$V.S = cte \quad (1)$$

##### 3.2.2. Flow equation

$$\frac{\partial V}{\partial t} = -\frac{1}{\rho_0} \frac{\partial P}{\partial r} - J.g - \frac{\rho}{\rho_0} g \sin \alpha \quad (4)$$

Where

$$J = \frac{f \cdot V^2}{2D \cdot g}$$

J is the pressure drop per unit length and f the factor of friction.

### 3.2.3. Heat equation

A heat balance of the collector and the chimney is required.

#### ➤ Heat balance for the collector

Considering the above assumptions for an elementary control volume of the collector, the following Figure (Fig.2) illustrates the mechanism of heat exchange.

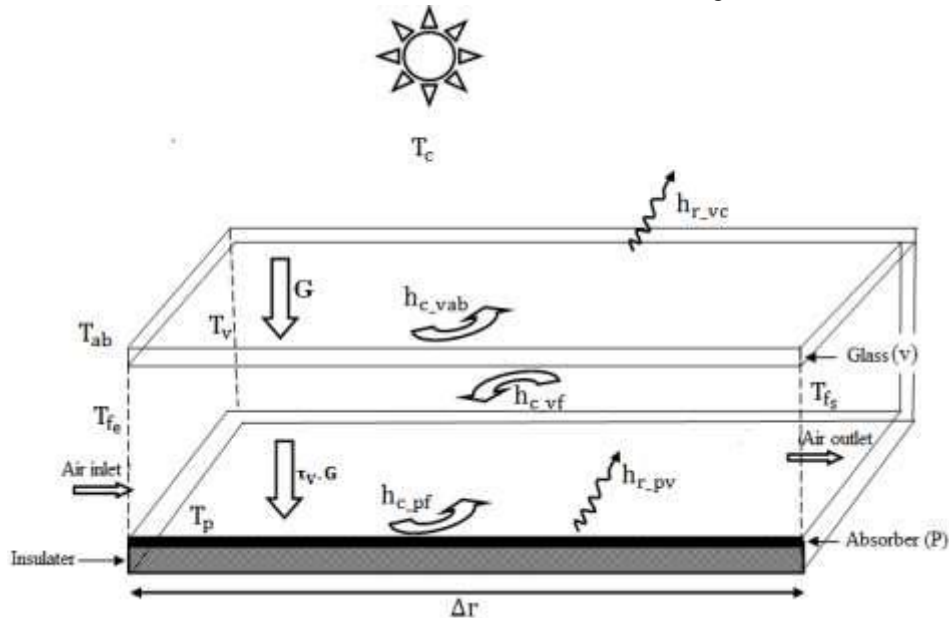


Fig.2: Illustration diagram of the different heat exchanges in the collector

#### ✓ Thermal balance of the glass

For an elementary surface and space  $\Delta r$  directed towards the center of the chimney, we get the following equation (6):

$$m_v C_{pv} \frac{\partial T_v}{\partial t} = -S_v h_{c,vab} (T_v - T_{ab}) - S_v h_{r,vc} (T_v - T_c) - S_v U_{av} (T_v - T_{ab}) + S_v h_{c,vf} (T_f - T_v) + S_p h_{r,pv} (T_p - T_v) + S_v \alpha_p \tau_v G$$

#### ✓ Thermal balance of the absorber

The solar energy received by the absorber is the difference between that transmitted by the surface of

#### ➤ Heat balance of the drying chamber or chimney

The various modes of heat exchange for a section of the fireplace are show in (Fig. 3).

the glass and that transferred to the fluid, including losses.

$$m_p C_{pp} \frac{\partial T_p}{\partial t} = -S_p h_{c,pf} (T_p - T_f) - S_p h_{r,pv} (T_p - T_v) - S_p U_{ar} (T_p - T_{ab}) + S_p \alpha_p \tau_v G$$

#### ✓ Thermal balance of the fluid (air)

The heat balance of the fluid inside the chimney is given by the following equation:

$$m_f C_{pf} \frac{\partial T_f}{\partial t} = -S_v h_{c,vf} (T_f - T_v) + S_p h_{c,pf} (T_p - T_f) - \dot{m}_f S_f (T_{fe} - T_{fs}) \quad (6)$$

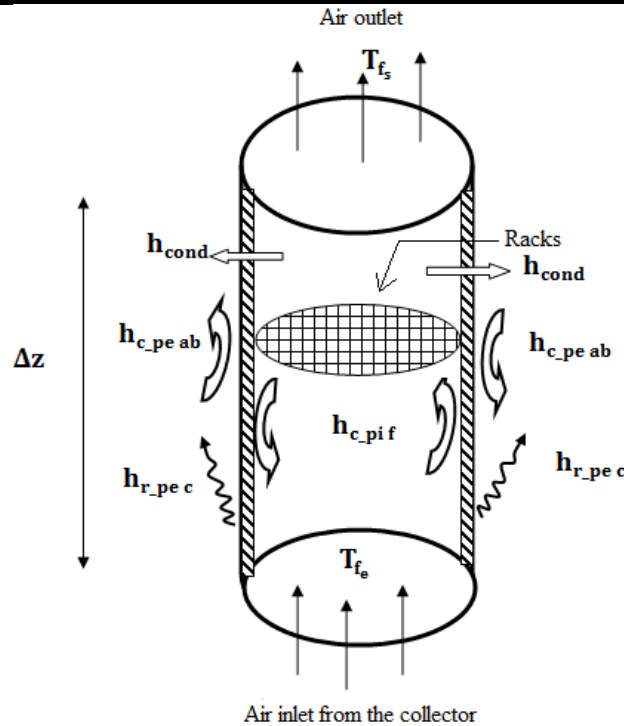


Fig.3: Illustration diagram of the different thermal exchanges in the drying chamber

- ✓ Thermal balance of the outer wall (pe)
 
$$m_{pe} C_{ppe} \frac{\partial T_{pe}}{\partial t} = -S_{pe} h_{c_{pe ab}} (T_{pe} - T_{ab}) - S_{pe} h_{r_{pe c}} (T_{pe} - T_c) + S_{pe} h_{cond} (T_{pi} - T_{pe}) \quad (9)$$
- ✓ Thermal balance of the inner wall (pi)
 
$$m_{pi} C_{ppi} \frac{\partial T_{pi}}{\partial t} = S_{pi} h_{c_{pi f}} (T_f - T_{pi}) - S_{pi} h_{cond} (T_{pi} - T_{pe})$$

- ✓ Thermal balance of the air in the drying chamber  
Heat exchanges related to the air are described by the following equation:

$$m_f C_{pf} \frac{\partial T_f}{\partial t} = -S_{pi} h_{c_{pi f}} (T_f - T_{pi}) - \dot{m}_f S_f (T_{fe} - T_{fs})$$

### 3.3 Coefficients of thermal exchanges

#### 3.3.1. Coefficients of exchanges by convection

- The coefficient of convective heat exchange between the environment air and the upper wall of the glass is given by Mc Adams equation (1954) [4]:

$$h_{c_{vab}} = 5.67 + 3.86 V_{vent}$$

- For that between the fluid and the bottom wall of the glass, we have the expression:

$$h_{c_{vf}} = \frac{Nu \lambda_f}{L_c}$$

- For that between the absorber and the fluid, we have the same expression as the previous one:

$$h_{c_{pf}} = \frac{Nu \lambda_f}{L_c}$$

#### 3.3.2. Coefficients of exchange by radiation

- Coefficient of radiative exchange between the glass and the sky:

$$h_{r_{vc}} = \sigma \epsilon_v (T_v + T_c) (T_v^2 + T_c^2)$$

With Swinbank relationship [5]

$$T_c = 0,0552 T_{ab}^{1.5}$$

- Coefficient of radiative exchange between the glass and the absorber:

$$h_{r_{pv}} = \frac{\sigma (T_v + T_p) (T_v^2 + T_p^2)}{\frac{1}{\epsilon_v} + \frac{1}{\epsilon_p} - 1}$$

- Coefficient of radiative exchange between the chimney and the sky:

$$h_{r_{pe c}} = \sigma \epsilon_{pe} (T_{pe} + T_c) (T_{pe}^2 + T_c^2) \quad (18)$$

#### 3.3.3. Coefficients of loss

- Loss ratio before the collector

$$U_{av} = h_{c_{vab}} + h_{r_{vc}}$$

- Coefficient of rear losses of the collector

$$U_{av} = \frac{1}{\frac{\epsilon_p}{\lambda_p} + \frac{\epsilon_{isolant}}{\lambda_{isolant}} + \frac{\epsilon_{plaque}}{\lambda_{plaque}} + \frac{1}{h_{c_{vab}}}} \quad (20)$$

### 3.4. Correlations for calculating the Nusselt Number (12)

Nusselt number depends on the Prandtl number and Grashof number or Rayleigh number ( $R_a$ ) in natural convection.

The absorber and the glass being horizontal plates heated from above, the Nusselt number of equations (11) and (12) is determined through the following correlations [6]. (13)

$$Nu = 0.54 R_a^{0.25} \quad (21) \quad (14)$$

With  $2 \cdot 10^4 < R_a < 8 \cdot 10^6$

$$Nu = 0.15 R_a^{0.33} \quad (23)$$

$$\text{With } 8 \cdot 10^6 < R_a < 8 \cdot 10^{11} \quad (24)$$

### 3.5. Choice of the method of resolution

To solve the equations of the system, we made the choice of the method of numerical solution with explicit finite differences. Using the method by slice, the system is divided into several dummy slices in the direction of the air flow.

## IV. RESULTS AND DISCUSSION

### 4.1. Materials and methods

The experiment took place on June 30, 2016 from 9 to 17 o'clock. We used a temperature logger named midi-logger with ten lanes equipped with Type K thermocouples for measuring the temperatures of the glass, absorber, drying air in the collector and the chimney. A radiometer and an anemometer allowed us to measure respectively the solar radiation of the day and the air speed at the exit of the chimney. The figure (Fig.4) below shows a photo of the experimental device.

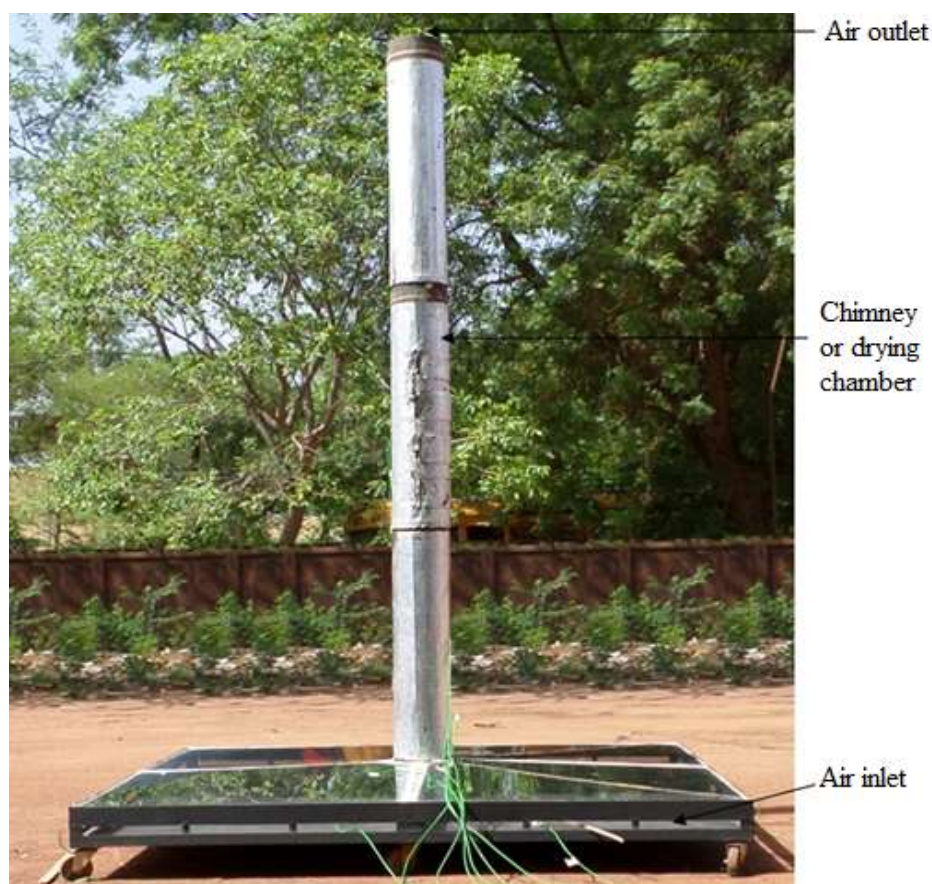


Fig.4: Photo of the experimental device

### 4.2. Comparison of theoretical and experimental global solar radiation

The following figures (Fig.5) and (Fig.6) respectively show the variation of the theoretical and experimental global solar radiation depending on the time of day on 30 June 2016 in Ouagadougou.

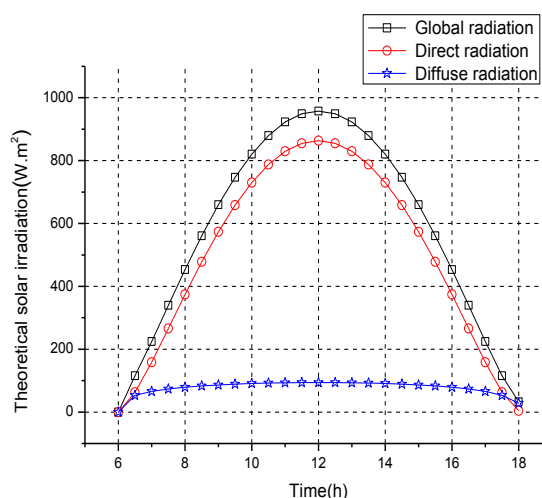


Fig.5: Theoretical variation in solar radiation



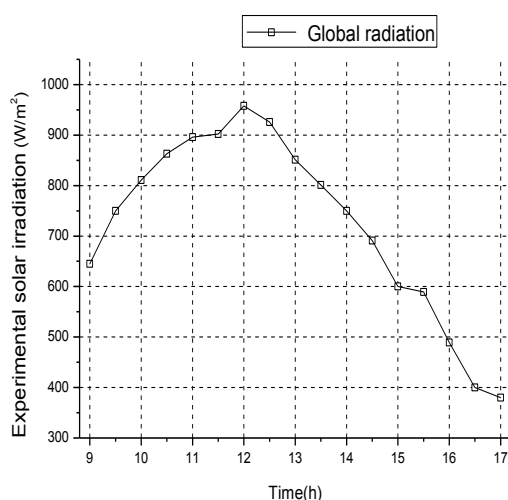


Fig.6: Experimental Variation of solar radiation

The manipulation began around 09 o'clock and we already saw a flux of  $650\text{W/m}^2$  slightly lower than that theoretically expected to be  $700\text{W/m}^2$  at the same time. Then this flow increases to reach its peak of  $950\text{W/m}^2$  at noon. We observe a sinusoidal growth in theory but the peak at 12 o'clock is  $967\text{W/m}^2$ . Some cloud passages were observed in the said day. The average systematic error (RMSE) between the theoretical and experimental values is about  $56\text{W/m}^2$ .

#### 4.3. Experimental and simulation results of the collector

##### 4.3.1. Results presentations

Figures (Fig.7) and (Fig.8) show the variation of the average temperatures of the glass, air and absorber as a function of time.

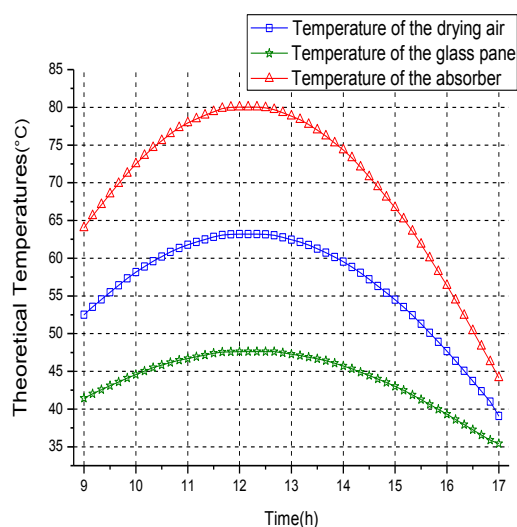


Fig.7: Theoretical temperature of the air, the glass and the absorber in the collector

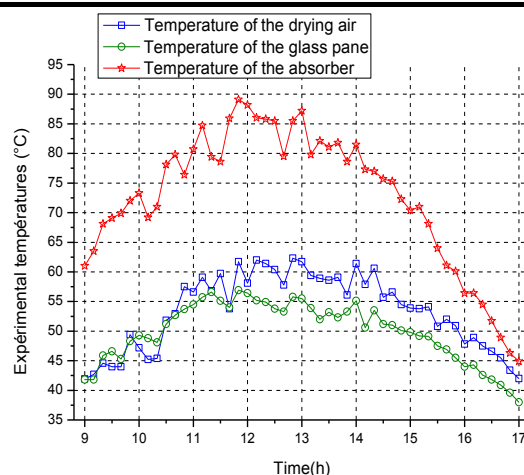


Fig.8: Experimental temperatures of air, glass and absorber in the collector

The various average temperatures of the absorber are superior to those of the air and glass respectively. We find that the temperatures rise gradually as solar radiation increases to maximum values between 12 o'clock and 13 o'clock. The theoretical maximum temperature of the absorber is  $81^\circ\text{C}$  against  $88^\circ\text{C}$  in practice. That of the glass is  $49^\circ\text{C}$  against  $55^\circ\text{C}$  and that of the air  $63^\circ\text{C}$  against  $62^\circ\text{C}$ .

##### 4.3.2) Comparison between the various temperatures of the air at the outlet of the collector

To validate our results, a comparative study was carried out with experimental and theoretical results. The figure (Fig.9) below shows us that comparison.

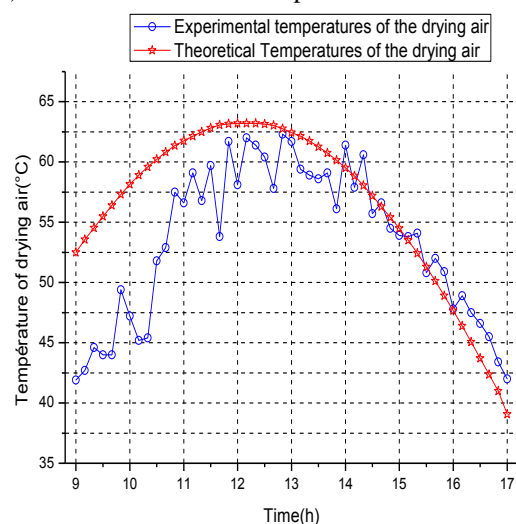


Fig.9: Comparison of experimental and theoretical temperature of the drying air

From 9 o'clock to 13.50, we see that the predicted temperatures are higher than the experimental temperatures while from 17 o'clock to 14 o'clock, experimental temperatures are slightly higher than those of the simulation. They increase or decrease according to the sunlight of that day and reach a maximum value of

about 62 ° C for the experimental temperature, and about 63 ° C for the simulated one with RMSE = 5.85 ° C. This same observation was made by al Hakim and sowed in 2013, when he simulated a solar tower with and without storage system. [7]

The temperature of drying air obtained at the outlet of the chimney enables the drying of certain food products whose drying temperatures do not exceed 62 ° C.

#### 4.4. Temperature Fields at the level of the racks

The average temperatures of the drying air at the racks are given in Figures (Fig.10) and (Fig.11). They respectively show theoretical and experimental temperatures at the four racks in function of time.

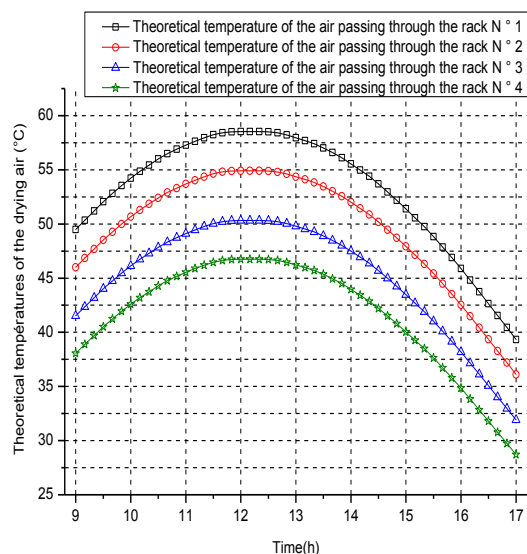


Fig.10: Theoretical average temperature of hot air in racks

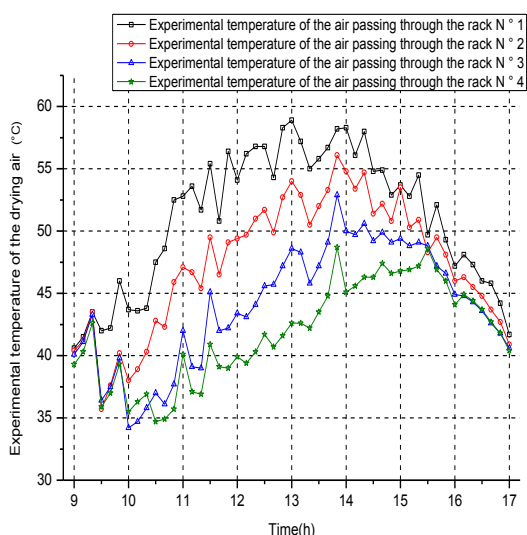


Fig.11: Experimental mean temperature of hot air at the racks

The temperature of the drying air at the racks also depends on sunshine. Rack N° 1 is traversed by a flow of hot air of higher temperature compared to the others. We

notice a decrease in the temperature of the hot air at the level of the racks (from rack N° 1 to N° 4). Respectively it shows theoretical and experimental maximum temperature of:

- 58 ° C and 59 ° C for rack N° 1,
- 55 ° C and 56 ° C for rack N° 2,
- 51 ° C and 52 ° C for rack N° 3
- 47 ° C and 48 ° C for rack N° 4.

This decrease in air temperature was noted by O.

MOCTAR et al in 2015, when he stated that the air temperature in the chimney decreases gradually as the air is ascending.

This range of air temperature at the location of the racks will allow us to dry products such as okra, medicinal or flavor leaves, green peas etc. [5]

#### 4.5. Velocity field outlet of the chimney

In the design of solar dryer dimensions, the temperature of the drying air and humidity are certainly important, but so does the velocity of the air; hence the need to compare the simulated velocity to the experimental ones. Figure (Fig.12) shows us the comparison of theoretical and experimental speeds out of the chimney as a function of time.

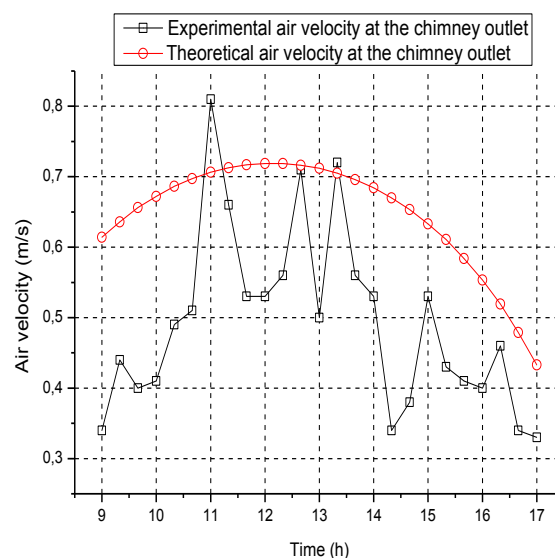


Fig.12: Comparison of experimental and theoretical speeds at the exit of the chimney.

The fluctuations of experimental velocity are due to the observed passages of cloud because these velocity also depend on sunlight. With a mean bias of 0.18 m / s, the maximum value of velocity measured at the outlet of the chimney or the drying chamber is 0.81m / s while that of the theoretical is in the range of 0.72m /s.

## V. CONCLUSION

Knowledge of the behavior of the airflow in the solar tower dryer is very important for the drying process. The range of theoretical and experimental temperatures at

different racks, tells us about the type of products to dry. Experimental velocity (0.81m / s) and theoretical (0.72m / s) out of the room to dry are low because our system works by natural convection. They have an impact on the drying time because they do not promote quick drying but can prevent the crusting of the product. These results will test the solar tower dryer by performing the drying of some agricultural products and improve our IT program to reduce average systematic errors.

### Nomenclature

S: Surface ( $m^2$ )

Cp: Specific heat at constant pressure ( $kJ \cdot kg^{-1}K^{-1}$ )

g: Acceleration of gravity ( $m \cdot s^{-1}$ )

G: Golar radiation ( $m \cdot s^{-1}$ )

m: Mass (kg)

h: Heat transfer coefficient  $W \cdot m^{-2}$

$\dot{m}$ : Mass flow ( $kg \cdot s^{-1}$ )

R: radius of collector m

P: pressure (Pa)

Nu: Nusselt Number

T: Temperature (K)

V: velocity ( $m \cdot s^{-1}$ )

dr: Variable Radius

dz: Variable height

e: Thickness (m)

U: Loss Factor  $W \cdot m^{-2}$

J: losses

f: friction factor

### Greek symbols

$\lambda$ : Thermal conductivity ( $W \cdot m^{-1}K^{-1}$ )

$\tau$ : Transmissivity

$\varepsilon$ : Emissivity

$\rho$ : Density of the air mass ( $kg \cdot m^{-3}$ )

$\sigma$ : Stefan-Boltzmann constant  $W \cdot m^{-2}K^{-4}$

$\beta$ : Coefficient of thermal expansion ( $K^{-1}$ )

### Indices

ab: Ambient

p: Absorber

f: fluid (air)

v: Glass window

av: Front window

RMSE: average bias

### REFERENCES

- [1] I. Cabanyes, "Proyecto de motor solar, la energia eléctrica", Revista general de electricidad y sus aplicaciones, Vol 8, pp. 61-65, 1903.
- [2] S. Roozbeh, A. Majid, H. Behzad, " Modeling and numerical simulation of solar chimney power plants", Solar Energy, Vol. 85, pp. 829–838 , May 2011.
- [3] M. Ousmane, B. Dianda, S. Kam, "Experimental study in natural convection", Global journal of pure and applied sciences, Vol 21, pp. 155-169, 2015
- [4] M. Daguenet, Les séchoirs solaires : théorie et pratique. Unesco, 1985.
- [5] K. Swinbank. "Thermal performance of solar air heater: Mathematical model and solution procedure solar energy", vol 55, 1995.
- [6] A. Yunus Cengel, J. Afshin Ghajar, "Heat and Mass Transfer: Fundamentals & Applications." McGraw-Hill, 2011, p. 567.
- [7] H. Semai and A. Bouhdjar , " Modélisation d'une centrale à cheminée solaire en régime turbulent et avec stockage thermique ", 16<sup>ème</sup> journée internationale de thermique.